

激光焊接不锈钢微间隙焊缝偏差角点检测法

高向东, 黄健源, 莫 玲
(广东工业大学 机电工程学院, 广州 510006)



高向东

摘 要: 针对大功率(10 kW)光纤激光焊接304不锈钢紧密对接微间隙焊缝(焊缝间隙小于0.1 mm),通过高速相机摄取熔池近红外热像并分析其特征,分析和处理熔池热像特征,提取激光束偏离焊缝位置的信息,探索激光束与焊缝偏差的信息表征。利用激光深熔焊的匙孔效应,研究焊缝在固态与液态交界处不稳定边缘特征点,提出一种角点检测法实现微间隙焊缝偏差的检测。结果表明,熔池红外热像角点密集分布中心与焊缝偏差有密切的关系,通过角点分布密度可以有效判断焊缝偏差状态。

关键词: 大功率光纤激光焊; 近红外热像; 焊缝偏差; 角点检测

中图分类号: TG409 **文献标识码:** A **文章编号:** 0253-360X(2013)12-0001-04

0 序 言

激光焊接具有能量密度高、热影响区小、焊接效率高等优点。在热能传递的过程中,熔池红外辐射蕴含着丰富的焊接状态信息,包括激光束偏离焊缝的状态。激光焊接对焊缝跟踪精度要求较高,等厚对接焊小于0.1 mm微间隙焊缝的检测和跟踪目前还没有得到很好的解决。传统的焊缝检测法一般基于结构光三角测量原理,根据横跨于焊缝的结构光的形变实现焊缝的检测^[1]。由于横跨于微间隙焊缝的结构光几乎形变极小,因此难以检测微间隙焊缝。为此,可通过熔池温度分布检测微间隙焊缝偏差^[2]。当激光束偏离焊缝中心时,焊缝两侧的热分布不均匀,通过匙孔形态可得到激光束与焊缝偏差的关系。由于焊缝间隙很小,因此采用熔池红外热像获取焊缝偏差方法的可靠性还需进一步研究和提高。

激光束的能量密度极高,匙孔处金属材料在极短的时间内从固态瞬间熔化和气化^[3],所以在金属材料固态与液态的交界处存在不稳定的气化现象,加上焊缝间隙的存在,液态金属会渗入焊缝间隙,反映在熔池红外热像上为不稳定的毛刺。这些现象与焊缝中心位置有着密切的关系。熔池红外辐射信号与焊接参数存在必然关联^[4],研究熔池红外热像特

征可探索焊缝信息。为此提出一种基于熔池红外热像角点的焊缝位置偏差检测方法,研究角点分布密度与焊缝中心位置的关系,探索通过角点法有效检测微间隙焊缝位置。在文献[2-5]的基础上,进一步研究突出焊缝位置信息的方法,为精确的焊缝检测和跟踪控制提供理论和试验依据。

1 试验方法

焊接试验装置包括松下6关节机器人,IPG YLR-40000大功率光纤激光器,NAC高速摄像机,拍摄速度1 000 f/s,试件为两块150 mm×49 mm×10 mm的304奥氏体不锈钢板,焊缝间隙小于0.1 mm。激光焊接试验装置结构如图1所示。表1为焊接试验条件^[2]。

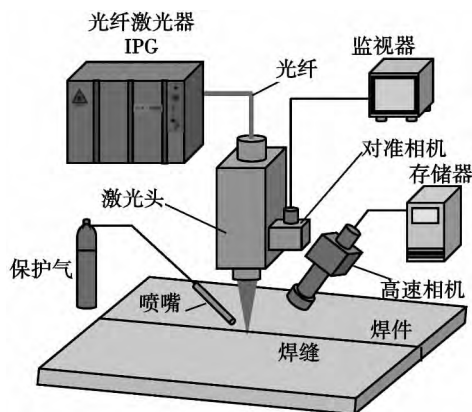


图1 大功率光纤激光焊接试验装置结构图

Fig. 1 Experimental setup of high power fiber laser welding

收稿日期: 2013-06-27

基金项目: 国家自然科学基金资助项目(51175095);广东省自然科学基金资助项目(10251009001000001, 9151009001000020);高等学校博士学科点专项科研基金资助项目(20104420110001)

表 1 大功率光纤激光焊接试验条件

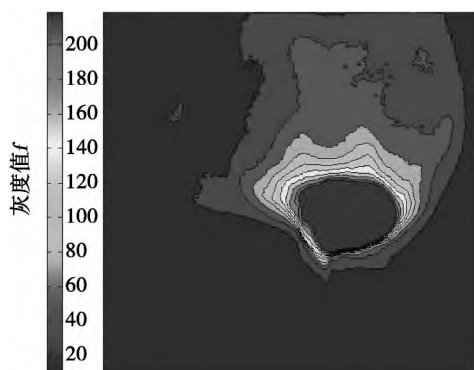
Table 1 Experimental conditions of high-power fiber laser butt joint welding

激光功率 P/kW	光斑直径 $D/\mu\text{m}$	焊接速度 $v/(\text{m}\cdot\text{min}^{-1})$	保护气体流量 $Q/(\text{L}\cdot\text{min}^{-1})$	摄像机波长 λ/nm
10	200	2.5	20	960~990

试验采用氩气作为保护气体,防止金属蒸气云的累积和空气的污染。为有效摄取熔池表面红外辐射,并滤除飞溅和金属蒸气云的辐射干扰,高速摄像机采用 960~990 nm 近红外波段。

2 熔池红外热像特征

试验获取的熔池红外热像分辨率为 512 像素 \times 512 像素,如图 2 所示。图 2a 为一幅熔池图像的等温分布,可看出匙孔为近圆形,焊缝间隙处有凸出特点,在待焊金属母材和匙孔交界处的轮廓线非常密集,焊缝间隙处也有突出的轮廓线。



(a) 熔池等温分布



(b) 滤波后效果

图 2 熔池红外热像处理

Fig. 2 Infrared image processing of molten pool

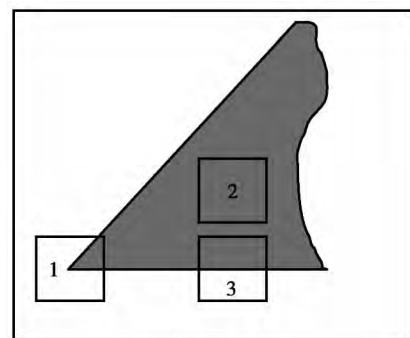
2.1 熔池热像预处理

首先对熔池区域图像进行滤波去除噪声,这里选取双边滤波器,在不削弱边缘信息的前提下有效

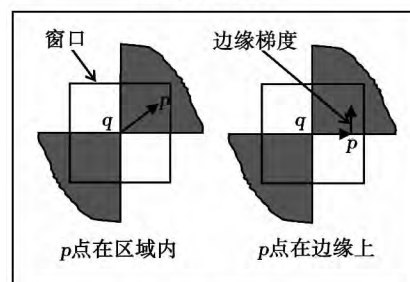
地滤除噪声。双边滤波器不仅考虑了像素点间的空间距离,还考虑了灰度值的相似性,所以它在边缘附近的滤波窗口是动态调整的,能较好地解决其它滤波器(如高斯滤波器)导致的边缘模糊问题^[6]。截取图 2a 的典型区域并对其双边滤波,其滤波效果如图 2b 所示。

2.2 角点检测

角点的基本概念由 Harris 提出,若一个像素点周围存在至少两个不同方向的纹理(边缘),则该点可视为角点^[7-8]。如图 3a 所示,角点检测的基本思想为:一个窗口在角点处沿任意方向移动时,窗口的灰度值之和变化均很大(窗口 1),而在平坦区域沿任意方向移动灰度和变化很小(窗口 2),沿边缘方向移动时灰度和变化也很小(窗口 3)。熔池图像角点检测采用 Shi-Tomasi 角点检测法,其为基于 Harris 改进的角点检测算法。使用 Shi-Tomasi 角点检测方法得到角点位置后,为了得到更精确的角点位置,需要计算亚像素级的角点位置。如图 3b 所示^[6],设初始角点 q 在亚像素级角点附近, p 为窗口内任意点(不包括 q)。检测所有 qp 向量,当 p 位于平滑区域时, p 处的梯度为 0;当向量 qp 的方向与边缘的方向一致时, p 的梯度方向与向量 qp 正交。以上情况 p 处的梯度与向量 qp 的点积都为零。在 p 周围可以得到多组梯度及相应的向量 qp ,令它们的点积为零,可以通过求解方程组得到 q 的亚像素级精度的位置。



(a) 角点检测窗口



(b) 亚像素角点检测

图 3 图像角点检测原理

Fig. 3 Principle of image corner point detection

对图 2b 进行亚像素角点检测,共检测 36 个角点,得到的熔池红外热像角点分布如图 4 所示。在待焊接金属边缘和焊缝间隙处,角点分布较密集,已焊接区域的角点分布很少。

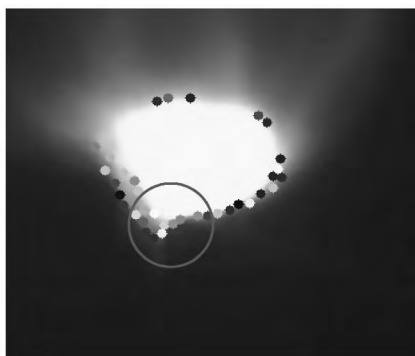


图 4 熔池亚像素角点分布

Fig. 4 Distribution of sub-pixel corner of molten pool

3 角点分布密度与焊缝中心位置

从图 4 中可以看到角点在焊缝间隙中心分布最为密集,且呈现锥形分布,利用该特点可以提取焊缝的中心位置。具体方法为,以每个角点为中心,统计以 40 像素为半径范围内角点的个数(图 4 圆圈内),并从多到少排列。如果角点个数最多的中心角点与上一时刻的焊缝中心位置差值小于 8 像素,则认为是当前时刻的焊缝中心位置,否则考虑角点个数第二多的中心角点,并依次比较直到找到符合要求的角点作为焊缝中心位置。针对激光束与焊缝对中及偏离情况,选取第 1 000 ~ 2 600 幅图像测量的焊缝中心位置如图 5 所示。

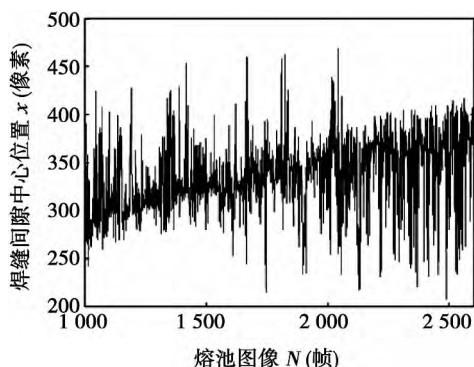


图 5 焊缝中心位置测量值

Fig. 5 Measured values of welding seam center

由图 5 可见,随着激光束对中和逐渐偏离焊缝,焊缝中心位置的测量值呈现递增趋势。

4 试验结果与分析

4.1 焊缝位置角点测量分析

焊接后的焊件实物如图 6a 所示,激光束焊接方向从左往右,焊接起始点(对应第 153 幅图像)右偏焊缝中心 $943\text{ }\mu\text{m}$,沿直线行进并斜跨焊缝,终止点(对应第 2 964 幅图像)左偏离焊缝中心 $705\text{ }\mu\text{m}$ 。激光束对中焊缝时对应第 1 803 幅图像,此时焊缝偏差为零。图 6b 中虚线为激光束与焊缝的偏差测量值(对应第 1 000 ~ 2 600 幅图像),使用窗口为 50 的加权滤波方法对焊缝偏差测量值进行平滑处理,结果如图 6b 中实线所示。

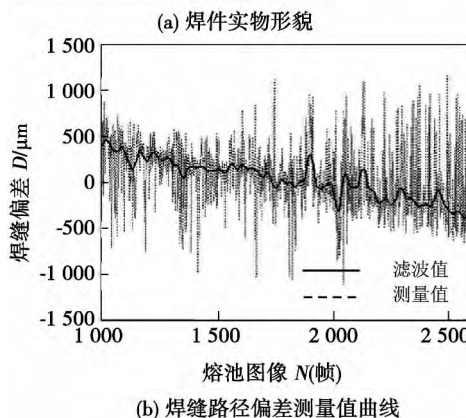
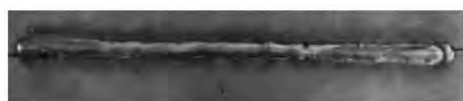


图 6 焊件实物与焊缝路径偏差测量值

Fig. 6 Bead surface of weldment and measured values of welding seam path deviation

4.2 焊缝偏差测量值的精度分析

激光头与高速像机的位置相对固定,图像中激光束中心位置坐标(像素)为(341.7, 277.3),图像尺寸为 512 像素 \times 512 像素,图像分辨率 114 像素/mm。偏差值为正表示激光束右偏焊缝,为负则表示左偏焊缝。为了检验角点检测法提取焊缝中心位置的精度,则须将焊缝偏差测量值与焊缝实际偏差值进行比较。

激光束与焊缝之间的实际偏差已知,焊缝路径偏差测量值减去实际值后得到测量误差,如图 7 所示。可看出采用角点方法测量焊缝偏差的精度较高。图 7 中虚线为由标准差值描述的对均值(点划线)的离散度。表 2 为焊缝路径偏差测量值的误差有关统计结果,焊缝路径偏差测量值的误差均值为 0.0494 mm 。采用角点检测方法能较准确地检测焊

缝中心位置,测量误差大多在 $\pm 200 \mu\text{m}$ 之间,能达到实际焊接过程控制的精度要求.焊缝偏差测量值的误差较大处主要由飞溅干扰所致,此时焊缝被飞溅遮挡从而导致测量值发生较大偏差.

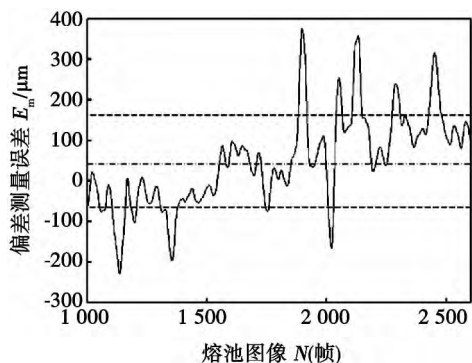


图 7 焊缝偏差测量值的误差曲线

Fig. 7 Measurement value errors of weld seam deviation

表 2 焊缝路径偏差测量值的误差统计分析

Table 2 Statistical analysis of measured value errors of weld seam path deviations

熔池图像统计 范围 N (帧)	中值 $M/\mu\text{m}$	均值 $A/\mu\text{m}$	方差 $S/\mu\text{m}$	最大值 $D_{\max}/\mu\text{m}$	最小值 $D_{\min}/\mu\text{m}$
1 000 ~ 2 600	42.7	49.43	113.3	375.4	-229.4

采用高速摄像机的目的是为了捕捉熔池的瞬态特征,更好地分析角点分布与焊缝位置之间关系.在实际焊接过程中可适当降低图像采样速率,满足焊接控制的实时性要求.

5 结 论

(1) 大功率光纤激光焊接熔池的红外辐射包含焊缝位置信息.采用高速像机能有效捕捉相关红外特征,通过分析和处理熔池热像能够提取到激光束偏离焊缝位置的信息.

(2) 角点检测方法可以检测到熔池的关键特征点,且角点分布与焊缝中心存在着密切的关系.根据角点分布情况能较准确地计算和检测微间隙焊缝

的中心位置,为大功率光纤激光焊接路径偏差测量提供了新方法.

致谢:

感谢日本大阪大学接合科学研究所片山实验室提供的焊接试验帮助.

参考文献:

- [1] Huang Wei, Kovacevic R. Development of a real-time laser-based machine vision system to monitor and control welding processes [J]. International Journal of Advanced Manufacturing Technology, 2012, 63(1/4): 235-248.
- [2] 高向东,游德勇, Katayama Seiji. 大功率光纤激光焊焊缝跟踪偏差测量新方法[J]. 焊接学报, 2011, 32(5): 49-52.
Gao Xiangdong, You Deyong, Katayama Seiji. A new approach to measure deviation of seam tracking in high-power fiber laser welding [J]. Transactions of the China Welding Institution, 2011, 32(5): 49-52.
- [3] Howard B C, Scott C H. 现代焊接技术[M]. 陈茂爱,王新洪,陈俊华,等,译. 北京: 化学工业出版社, 2010.
- [4] 高大新,段爱琴,孟亮,等. CO_2 激光焊接 TA15 熔池红外光辐射信号与焊接参数的关系[J]. 焊接学报, 2012, 33(6): 89-92.
Gao Daxin, Duan Aiqin, Meng Liang, et al. Relation between relative intensities of infrared radiation and welding parameter during CO_2 laser welding of TA15 [J]. Transactions of the China Welding Institution, 2012, 33(6): 89-92.
- [5] 高向东,莫玲,游德勇,等. 焊缝偏差 RBF 神经网络预测算法[J]. 焊接学报, 2012, 33(4): 1-4.
Gao Xiangdong, Mo Ling, You Deyong, et al. Prediction algorithm of weld seam deviation based on RBF neural network [J]. 2012, 33(4): 1-4.
- [6] 王玉灵. 基于双边滤波的图像处理算法研究[D]. 西安: 西安电子科技大学, 2010.
- [7] Ryu J B, Park H H. Log-log scaled harris corner detector[J]. Electronics Letters, 2010, 46(24): 1602-1604.
- [8] Bradski G, Kaehler A. 学习 OpenCV[M]. 于仕琪,刘瑞祯,译. 北京: 清华大学出版社, 2009.

作者简介: 高向东,男,1963 年出生,教授,博士研究生导师.主要从事焊接自动控制研究工作.发表论文 150 余篇. Email: gaofd666@126.com

MAIN TOPICS ,ABSTRACTS & KEY WORDS

Detection of seam deviation of micro butt gap in laser welding of 304 austenitic stainless steel based on corner point method

GAO Xiangdong , HUANG Jianyuan , MO Ling (School of Electromechanical Engineering , Guangdong University of Technology , Guangzhou 510006 , China) . pp 1 - 4

Abstract: Infrared radiation from the molten pool contains plenty of welding status information including the characteristics of the seam deviation. Infrared images of the molten pool were captured by an infrared sensitive high-speed camera during high power (10kW) fiber laser butt joint welding of 304 austenitic stainless steel with micro-gap seam (seam gap width was less than 0.1mm) . By analyzing the molten pool characteristics , the information of seam deviation was explored. A keyhole formed when the laser beam was focused on a weldment and the metal vaporized instantly. Features of the keyhole infrared images , especially the characteristics of conjunction between the solid and liquid zones with unstable burr edge of seam were studied. A corner point detection method was proposed to detect the micro-gap seam deviation in high power laser welding process. Experimental results showed that the dense distribution center of the corner points of a molten pool infrared image had a close relationship with the weld seam deviation. The micro-gap weld seam deviation status in high power fiber laser welding can be determined by the corner point distribution density.

Key words: high power fiber laser welding; near infrared thermal image; seam deviation; corner point detection

Embedded system control of consumable DE-GMAW

SHI Yu¹ , WANG Ping² , GUO Jinchang² , FAN Ding¹ (1. State Key Laboratory of Gansu Advanced Non-ferrous Metal materials , Lanzhou University of Technology , Lanzhou 730050 , China; 2. Welding Team of Process Department in Dongfang Electrical Machinery Co. , Ltd. , Deyang 618000 , China) . pp 5 - 8

Abstract: By applying the embedded system control to carry out the control tests for consumable DE-GMAW , the welding process is unstable , main arc and bypass arc are affected each other , bypass arc length is unstable , bypass current changes seriously , and there is welding defects and poor weld appearance in open loop welding. Stability test of the welding process based on the arc voltage feedback prove that the embedded system can feedback arc voltage in real time , adjust bypass wire feeding rate and control the bypass arc length , make sure welding process stable. Stability test of the welding process based on the current control shows that the embedded system can feedback the bypass current in real time , judge the bypass current change trend , adjust the bypass current in real time , ensure current in base metal to be stable. Applications of the embedded system control of both bypass wire feeding and bypass current ensure stable welding process , avoidance of welding defect and good weld appearance.

Key words: embedded system; consumable DE-GMAW;

arc voltage feedback; control current

Parameter optimization for MAG of DP780

LU Zhenyang , TANG Chao , XIONG Wei , HUANG Pengfei (Welding Institute , Beijing University of Technology , Beijing 100124 , China) . pp 9 - 12

Abstract: Gas metal arc welding parameters were optimized by orthogonal experiments for 2mm thick uncoated DP780 steel plate. The influences of five factors including wire feeding rate , welding speed , arc voltage , wire extension and welding angle on tensile strength of DP780 lap joints were discussed. The range analysis and variance analysis proved that wire feeding rate and welding speed are the main influencing factors on the tensile strength of the join , and the other factors show no regularity to tensile strength. An approximate mathematical model to control the tensile strength of the joint was obtained by fitting the approximate curve through multiple regression analysis , which revealed the regularity of effects of main welding parameters on the tensile strength of the joint.

Key words: AHSS; MAG; process parameter optimization

A welding power supply with half-bridge LLC resonant soft-switching

CHEN Yanming¹ , YANG Meizhen¹ , WANG Zhenmin² , XUE Jiaxiang² , LI Guojin¹ (1. College of Electrical Engineering , Guangxi University , Nanning 530004 , China; 2. College of Mechanical Engineering , South China University of Technology , Guangzhou 510640 , China) . pp 13 - 16

Abstract: By using the magnetizing inductance of transformer , resonant capacitor and additional inductance , a half-bridge LLC resonant welding power supply with constant output voltage was implemented. Through careful analysis and design of relevant parameters (such as the series resonant inductor L_r , series resonant capacitor C_r , and the resonant inductor L_m paralleled with transformer etc) in the resonant tank , the ZVS turn-on can be achieved for primary side power switch , and the ZCS turn-off can be achieved for secondary rectifier diodes over the entire operation region. Hence , the loss and the interference can be decreased , the efficiency can be increased , the switching frequency can be higher so that the weight and the volume of the inductance , the capacitance and the transformer , and so on , can be decreased dramatically , and the dynamic behavior can be improved. The operation principle was also discussed briefly , a 2.5kW half-bridge LLC welding power supply was constructed and the experimental results were presented.

Key words: half-bridge LLC converter; resonant; Zero-voltage turn-on; Zero-current turn-off

Interface microstructure and mechanical properties of diffusion bonded joints between tungsten and ferritic steel with vanadium interlayer

MA Yunzhu , WANG Yanyan , LIU